

## **Why is the Bay of Bengal experiencing a reduced rate of sea surface warming?**

Joshua Rosario D'Mello<sup>a</sup> and S. Prasanna Kumar<sup>a,\*</sup>

<sup>a</sup> CSIR-National Institute of Oceanography, Dona Paula– 403 004, Goa, India.

\*Corresponding author: S. Prasanna Kumar; <sup>a</sup> CSIR-National Institute of Oceanography (CSIR-NIO), Dona Paula– 403 004, Goa, India.

E-mail: [prasanna@nio.org](mailto:prasanna@nio.org); Telephone: 91-832-2450300; Fax: 91-832-2450608

### **Abstract**

The sea surface temperature (SST) in the Bay of Bengal (BoB) during the period 1960 to 1995 showed a decadal cycle, riding over a warming trend. The disruption of the decadal cycle was noticed post-1995 and was followed by a slowdown in the sea surface warming. The cause for the disruption of the SST decadal cycle was the weakening of the link between SST and sunspot number. The rising trend in the sea surface temperature is due to the increasing atmospheric CO<sub>2</sub> concentration. The post-1995 SST slowdown was due to the increasing influence of the number of depressions, cyclones and severe cyclones in the Bay of Bengal, the occurrence of which showed an upward trend. Using Price-Weller-Pinkel model we show that cyclonic systems deepen the mixed-layer through enhanced mechanical-mixing with cooler sub-surface waters, thereby reducing the mixed-layer temperature and consequently the SST. This process opposes the SST rise due to increasing atmospheric CO<sub>2</sub> concentration. The net effect of the wind-mixing caused by the increased number of depressions, cyclones and severe cyclones and the increased CO<sub>2</sub> concentration is a SST slowdown in the Bay of Bengal. This mechanism differs from the SST slowdown mechanisms suggested for the Atlantic and the Pacific.

### **Key Points:**

- First report of the Bay of Bengal SST decadal cycle disruption and secular warming
- Decadal cycle disruption is due to weakening link between sunspot number and SST
- Post-1995 slowdown in SST warming linked to increased number of cyclonic systems
- Cyclonic wind-mixing with cool sub-surface water reduces the SST warming

**Keywords:** SST slowdown, Decadal cycle, Bay of Bengal, Wind-mixing, Ekman-pumping, Regional Climate Change, Sea Surface Temperature

## 1. Introduction

The Bay of Bengal (BoB), located in the eastern part of the northern Indian Ocean, has unique geographic and climatic setting. Being bound to its north ( $\sim 23^\circ\text{N}$ ) by the Asian landmass, the basin's water has no link to the polar waters. Besides, the basin's waters experience seasonal wind reversal associated with Asian monsoons, having south-westerly winds during summer monsoon (June to September) and north-easterly winds during winter monsoon (November to February). The south-westerly winds are generally warm and moist, while the north-easterly winds are cold and dry (Prasanna Kumar and Narvekar, 2005). In response to this reversal in wind direction the surface current also reverses in the basin. The BoB has one of the lowest surface salinities of the world oceans, which arises due to (1) excess evaporation over precipitation ( $\sim 2$  m/year) (Prasad, 1997) and (2) fresh water influx from adjoining rivers ( $1.625 \times 10^{12}$  m<sup>3</sup>/year) (Subramanian, 1993).

Seasonality being the dominant mode of variability in the BoB, seasonal cycle of hydrography and circulation is well researched and documented (see for e.g., McCreary *et al.*, 1993; Potemra *et al.*, 1991; Rao and Shivkumar, 2000, 2003; Schott and McCreary, 2001, Shankar *et al.*, 2002; Shetye *et al.*, 1996; Varkey *et al.*, 1996 and references therein). However, the slower modes such as multi-annual and especially the decadal variability are less explored, making our understanding of the long term variability of the Indian Ocean, in the context of climate change, rudimentary. In contrast there had been some studies pertaining to the slowdown in the SST warming in the Pacific and the Atlantic (Chen and Tung, 2014; Kosaka and Xie, 2013; McGregor *et al.*, 2014; Trenberth and Fasullo, 2013; Trenberth *et al.*, 2014) oceans. RupaKumar *et al.* (2002) was the first to show that the Indian Ocean was warming at the rate of  $0.5^\circ\text{C}$  per 100 years, based on the analysis of SST data during 1904 to 1994. Subsequently, Prasanna Kumar *et al.* (2009) showed that the Arabian Sea is experiencing a secular warming and a regional climate shift after mid-1990 based on analysis of SST data during 1960 to 2005. However, no such studies on long term variability are available in the case of the BoB. It is in this context that in the present study, using 52 years of SST data, we (1) examine the long-term SST trend, (2) decipher the recent change in the rate of warming, and finally (3) identify the factors responsible for the observed changes.

## 2. Materials and methods

### 2.1 Data

The Bay of Bengal ( $0^{\circ}$  -  $25^{\circ}$ N and  $80^{\circ}$ E-  $99^{\circ}$ E) SST, u-wind and v-wind components data were extracted from the International Comprehensive Ocean-Atmosphere Data Set (ICOADS) (Woodruff *et al.*, 2005) ([www.esrl.noaa.gov/psd/data/gridded/data.coads.1deg.html](http://www.esrl.noaa.gov/psd/data/gridded/data.coads.1deg.html)) for the period 1960 to 2011, having monthly mean values on a  $1^{\circ}$  by  $1^{\circ}$  spatial grid. Using the monthly mean SST data, a 60-month running mean was computed for further analysis. We used sunspot number as a proxy for the solar irradiance (Willson and Hudson, 1988) as the latter is available only from 1975. The monthly values of the international sunspot number (Solar Influences Data analysis Centre (SIDC) team, 2012), now available at <http://sidc.oma.be/sunspot-data/>, were obtained from [ftp://ftp.ngdc.noaa.gov/STP/SOLAR\\_DATA/SUNSPOT\\_NUMBERS/INTERNATIONAL/monthly/MONTHLY](ftp://ftp.ngdc.noaa.gov/STP/SOLAR_DATA/SUNSPOT_NUMBERS/INTERNATIONAL/monthly/MONTHLY). The annual mean global Carbon dioxide concentration data were obtained by merging the Carbon dioxide concentration at Mauna Loa from 1958 March to 1979 December ([ftp://ftp.cmdl.noaa.gov/ccg/co2/trends/co2\\_mm\\_mlo.txt](ftp://ftp.cmdl.noaa.gov/ccg/co2/trends/co2_mm_mlo.txt)) with the global Carbon dioxide concentration data from 1980 January to 2011 December ([ftp://ftp.cmdl.noaa.gov/ccg/co2/trends/co2\\_mm\\_gl.txt](ftp://ftp.cmdl.noaa.gov/ccg/co2/trends/co2_mm_gl.txt)) (Keeling *et al.*, 2001). Data on the number of depressions, cyclones and severe cyclonic storms (DCS) in the BoB was taken from e-atlas of India Meteorological Department available at <http://www.rmchennaieatlas.tn.nic.in/login.aspx?ReturnUrl=%2f> for the period 1960 to 2011.

The evaporation rate was taken from Objectively Analyzed Air-Sea Fluxes (OAFlux) (<http://dss.ucar.edu/datasets/ds260.1/>) (Yu *et al.*, 2008), while the precipitation rate was from the climate diagnostic centre (CDC) derived NCEP reanalysis products ([http://www.esrl.noaa.gov/psd/cgi-bin/db\\_search/](http://www.esrl.noaa.gov/psd/cgi-bin/db_search/)). The monthly gridded data of the short wave radiation, long wave radiation, latent heat flux and sensible heat flux were from the National Centres for Environmental Prediction/ National Centre for Atmospheric Research (NCEP/NCAR) Reanalysis Monthly Means and Other Derived Variables data (Kalnay *et al.*, 1996) and were obtained from (<http://www.esrl.noaa.gov/psd/data/gridded/data.ncep.reanalysis.derived.surfaceflux.html>).

For comparing the model mixed layer depth (MLD), the data on the MLDs were taken from Holte *et al.* (2010) (<http://mixedlayer.ucsd.edu/data/monthlyclim.nc>) and Keerthi *et al.* (2013) ([www.ifremer.fr/cerweb/deboyer/mld/Surface\\_Mixed\\_Layer\\_Depth.php](http://www.ifremer.fr/cerweb/deboyer/mld/Surface_Mixed_Layer_Depth.php)). In Holte *et al.* (2010) the

MLD climatology was computed using Argo profiles and a hybrid method (Holte and Talley, 2009), while in Keerthi *et al.* (2013) the monthly MLD data for the Indian Ocean, during 1969 to 2009 was based on temperature and salinity profiles taken from different sources namely National Oceanographic Data Centre (NODC) World Ocean Database 2009 (WOD 09), World Ocean Circulation Experiment (WOCE) global dataset version 3.0, Argo profile data and Tropical Atmosphere Ocean project Research moored Array for the African-Asian-Australian Monsoon Analysis and prediction (TAO RAMA) buoy daily data. Using this data monthly mean climatology (1969-2009) was computed for comparing with PWP model output.

Data used for plotting the schematic on SST cooling associated with the passage of cyclone Nargis during 27<sup>th</sup> April to 3<sup>rd</sup> May 2008 is as follows. The SST data is for 2<sup>nd</sup> May 2008 from NOAA daily Optimum Interpolation SST (OISST) obtained from <http://www.ncdc.noaa.gov/sst/griddata.php> (Reynolds *et al.*, 2007). The vertical temperature data along the 90°E (5-day average centred at 2<sup>nd</sup> May) and 1.5°S (5-day average centred at 3<sup>rd</sup> May) sections (<http://www.pmel.noaa.gov/tao/disdell/frames/main.html>) are from Research moored Array for African-Asian-Australian Monsoon Analysis and prediction (RAMA) moorings. Daily RAMA mooring data is also used to calculate the cooling by Cyclone Nargis, at the (15 °N, 90 °E) location. The cyclone track data is from [http://weather.unisys.com/hurricane/n\\_indian/2008H/NARGIS/track.dat](http://weather.unisys.com/hurricane/n_indian/2008H/NARGIS/track.dat)

## **2.2 Model**

### **2.2.1 Price-Weller-Pinkel (PWP) Model**

The Price-Weller-Pinkel (PWP) model (Price *et al.*, 1986) is a mixed-layer model similar to the dynamic instability model of Price *et al.* (1978), but modified to include mixing in the stratified fluid, below the mixed-layer. The model takes into account mixing processes namely (1) free convection arising due to surface heat loss, (2) mixed-layer entrainment by relaxation and (3) shear flow instability driven mixing. More details about the model and the data used to run it are given in the supporting information S1.

## **3. Results and Discussion**

The basin-averaged SST variability is examined to study the dominant variability during the study period from 1960 January to 2011 December. Then the role of the sunspot number and atmospheric CO<sub>2</sub> concentrations, are studied in the mediation of the observed changes. Finally, the PWP model helped to

show the mixed-layer deepening and cooling by cyclonic systems, to explain the reason for SST slowdown.

### **3.1 Decadal cycle and SST warming**

The salient feature, of the basin-averaged 60-month running mean monthly SST in the BoB, was a dominant decadal cycle riding over a secular warming trend of 0.014 °C per year (coefficient of determination,  $R^2= 0.88$ ) during the period 1960 to 2011 (Figure 1).

The second important feature was the disruption in the decadal cycle as well as the change in the warming trend after 1995. Note that 1995 November is the minimum of the 60-month running mean of the sunspot number cycles, occurring closest to the start of the disrupted SST cycle. Hence it has been chosen as the year for dividing the period of study in order to infer the warming trend. Thus, prior to 1995, the trend line of SST showed a warming with a slope of 0.015 °C per year ( $R^2= 0.79$ ), which slowed down to 0.008 °C per year ( $R^2= 0.35$ ), after 1995. All the three SST slopes have p-values lesser than 0.05 indicating a significance level of greater than 95%. The difference of the pre-1995 and post-1995 SST slopes also showed a similar p-value.

It has been shown that the natural decadal cycle is closely related to the solar activity (White, 1997). An examination of the sunspot number revealed a smooth decadal cycle that co-varied with SST until 1995 (Figure 1). After 1995, though the sunspot number cycle continued its decadal cycle without any disruption, the SST did not show a commensurate decrease with the decreasing sunspot number. In fact, SST continued to increase even when the sunspot number cycle started decreasing after 2000. A brief period of decrease in SST was noticed during 2004-2006, before the beginning of the next decadal cycle. Thus, we see a strong link between the decadal cycles of the SST and sunspot number until 1995. This link not only weakens after 1995, a slowdown of SST warming was also observed.

### **3.2 Correlation of SST with sunspot number and CO<sub>2</sub> concentration**

We explored the probable reasons for the observed disruption of decadal cycle and decline in the rate of warming in the BoB after 1995. The solar activity being the primary driver of the decadal variability in the ocean, we examined the correlation coefficient of SST with sunspot number cycle.

The correlation coefficient ( $r$ ) of the 60-month running means of sunspot number and SST in the various pre-1995 sunspot number cycle periods are high, with  $r = 0.66, 0.63$  and  $0.78$  (all significant at  $> 99.99\%$ ), for the periods centred from 1964 March to 1975 June, 1975 June to 1985 December and 1985

December to 1995 November respectively. During 1960 to 1995, when the SST showed an increase, the correlation coefficient with sunspot cycle was 0.58 (significance level > 99.99 %) and after 1995 it reduced to 0.24 (significance level = 99.82 %). Similarly, the correlation coefficient of SST with CO<sub>2</sub> was 0.88 (significance level > 99.99 %) during 1960 to 1995 period, which also declined to 0.54 (significance level > 99.99 %) for the period from 1995 to 2011. Thus, the reduced warming despite the increase in the CO<sub>2</sub> concentration after 1995 indicated that this could be due to reasons other than the CO<sub>2</sub> forcing. We now address the reasons for the reduced warming and identify the processes responsible for it.

### **3.3 Processes linked to the slowdown in warming**

The processes that could reduce the SST in the ocean are (1) upwelling, (2) evaporative cooling, (3) wind-driven/convective mixing and (4) Ekman-pumping. The BoB is not known for the prevalence of strong upwelling except for very localized regions close to the south-western boundary (Shetye *et al.*, 1991) and south of Sri Lanka (Vinayachandran and Yamagata, 1998), during summer monsoon. Evaporative cooling is a process which reduces the surface temperature consequent to the release of latent heat flux to the atmosphere. This could occur either due to an increase in wind speed, which is normally encountered during summer monsoon or with the prevalence of dry air blowing over the ocean as it occurs during winter monsoon (Prasanna Kumar and Narvekar, 2005). The wind-driven mixing, on the other hand, can cool the surface temperature of the ocean by mixing the warm upper ocean water with cold subsurface water through mechanical-mixing and deepening of mixed layer. This process could potentially lower the SST in the BoB during summer monsoon when the basin-wide wind speeds are the highest. However, though a basin-wide lowering of SST was noticed during summer monsoon the mixed-layer was not very deep, especially in the northern Bay, indicating the role of stratification in curtailing the wind-mixing (Narvekar and Prasanna Kumar, 2014). This points to the overriding role of wind in cooling the surface waters of the BoB through the latent heat loss. Convective mixing is a dominant mechanism of cooling of SST in the northern Arabian Sea, located in the western part of the northern Indian Ocean, during winter (Prasanna Kumar and Prasad, 1996). However, a similar process does not take place in the BoB due to the perennial presence of fresh water in the northern Bay.

Ekman-pumping is yet another process that is capable of bringing down the temperature of the upper ocean through cyclonic winds. The BoB is known for tropical cyclone activity which occurs regularly during spring-summer (April-June) and fall-winter (October-December) transitions. Tropical cyclones

induce intense cooling by both enhanced evaporation and vertical mixing under strong winds. Studies by Webster *et al.* (2005) showed that in the northern Indian Ocean category 4 and 5 cyclones have increased over the years, while Prasanna Kumar *et al.* (2009) based on the data from 1970 to 2007 in the Arabian Sea have showed a five-fold increase in the occurrence and intensity of the most intense cyclone (wind speed exceeded  $100 \text{ km h}^{-1}$ ).

An examination of the 5-year running mean of yearly total number of depressions, cyclones and severe cyclonic storms in the BoB showed an overall decreasing trend from 1960 to 2002 and thereafter it showed a sharp increase (Figure 2).

In order to decipher the relative roles of the above said processes in cooling the upper ocean waters in the BoB we have computed partial correlation of SST with wind speed (WS), net heat flux (NHF), evaporation minus precipitation (E-P) and the total number of DCS. Since the disruption in decadal cycle as well as slowdown in SST warming was noticed after 1995, we computed the partial correlation prior to and after 1995 and presented in Table 1.

The highest correlations of SST prior to 1995 were with NHF and E-P, which indicated that SST was controlled by latent heat loss through evaporative cooling. Note that though the number of DCS was negatively correlated its contribution was very small. In contrast, after 1995 the role of NHF and evaporative cooling diminished considerably, while the influence of number of DCS on SST increased. Thus, an increase in the number of DCS would lead to an enhanced cooling of surface waters through increased occurrence of upward-Ekman pumping. In addition, mechanical-mixing by the cyclonic winds would also lead to deepening of mixed-layer and thereby cooling of surface waters. In order to explore this, we used PWP-model (Price *et al.*, 1986). This model computes the vertical mixing, with the temperature and salinity profiles taken from World Ocean Atlas (WOA09) as initial conditions and forced by heat (NHF), momentum (wind-stress) and fresh water fluxes. The fresh water flux is computed as the difference of the evaporation from the sum of precipitation and river run-off (E-P-R). Our purpose of using a one-dimensional mixed-layer model is only to diagnose the role of wind-mixing under strong cyclonic conditions, similar to that of a sensitivity analysis approach, for identifying the process.

The model was run with the daily mean climatology for two years. The seasonal cycle of wind speed and model mixed-layer depth (MLD) from the 2<sup>nd</sup> year is presented in Figure 3.

The MLD, in general, co-varied with wind but inversely. The model MLD showed a bimodal distribution with shallow MLD during April and October coinciding with the periods of relatively weaker wind speeds. Note that the shallowest MLD was in April. The seasonal cycle of model MLD was similar to that obtained by Narvekar and Prasanna Kumar (2006) from in situ data, as well as those obtained from the data of Holte *et al.* (2010) and Keerthi *et al.* (2013), which gave us confidence in the model simulation. In order to assess the impact of cyclonic winds on the MLD during spring-summer and fall-winter transitions, the model was forced with wind speeds peaking to 63 km/hr (run 1), 87 km/hr (run 2) and 120 km/hr (run 3) in the second year of the runs (see supporting information S2). We see a deepening of the model MLD, both during spring-summer (Figure 4) and the fall-winter (Figure 5) transitions, which is similar to the Ekman depth calculated using scalar winds. This indicated that the mixed-layer deepening, which occurred under the influence of cyclonic winds, was through wind-mixing.

Thus, it is evident from the model run that strong winds associated with cyclones during both spring-summer as well as fall-winter transitions lead to deep mixed-layer through enhanced mechanical-mixing. This is depicted in the schematic diagram (Figure 6), which shows the SST cooling of approximately 1.5 °C to 2.5 °C, at (12 °N, 86 °E) location, associated with the passage of cyclone Nargis during 27<sup>th</sup> April to 3<sup>rd</sup> May 2008. The SST daily data, at the RAMA mooring location (15 °N, 90 °E) shows a maximum drop of 1.93 °C, from the 27<sup>th</sup> April 2008 to the 2<sup>nd</sup> May 2008, and a drop of 0.52 °C, in the period from the 27<sup>th</sup> April 2008 to the 11<sup>th</sup> May, 2008, showing that the cooling due to the cyclone lasts around 15 days.

We have also examined the actual observational data on mixed layer depth prepared by Keerthi *et al.* (2013) from 1969 to 2009. This data base for the Indian Ocean domain was assembled using all the measurements of mechanical bathythermographs (MBT), expendable bathythermographs (XBT), conductivity-temperature-depth (CTD) and profiling floats, besides Argo and RAMA moored buoys data. This MLD data also showed a deepening in the period from 1995 to 2009 (Figure 7).

Finally, to bring out the unique, relative contributions of CO<sub>2</sub> concentration, sunspot numbers and the number of DCS on the SST, a partial correlation analysis was carried out (Table 2).

The partial correlation of SST and sunspot number in the pre-1995 and post-1995 periods reduce from 0.76 (significance level > 99.99 %) to 0.2 (significance level = 99.03 %) respectively. This indicated the



decreased post-1995 influence of sunspot number on SST and we attribute this weakening link to be the cause for the disruption of the SST decadal cycle after-1995. In contrast to the sunspot number and SST partial correlation, the partial correlation coefficient of CO<sub>2</sub> concentration with SST increases from 0.47 (significance level > 99.99 %) to 0.82 (significance level > 99.99 %). Similarly, the partial correlation of SST and the number of DCS increases from -0.26 (significance level > 99.99 %) to -0.43 (significance level > 99.99 %). This shows that the link between the number of DCS and SST is stronger after-1995.

Though the sunspot number reduction, can cause some amount of fall in the rate of SST-rise i.e. the SST slowdown, the post-1995 influence of the sunspot number on SST is lesser than the post-1995 influence of the number of DCS on SST, as seen through their respective post-1995 partial correlation coefficients. Besides this, since the magnitude of the post-1995 partial correlation of CO<sub>2</sub> concentration and SST is greater than that of the number of DCS and SST partial correlation, we conclude that the influence of the CO<sub>2</sub> concentration is greater on the SST, compared to the number of DCS. However, the impact of the CO<sub>2</sub> concentration and number of DCS on SST, being generally opposite, the increase in the number of DCS though leading to enhanced cooling of the upper ocean, cannot completely offset the CO<sub>2</sub> driven warming. Thus, the above situation leads to a slowdown in SST warming in the BoB.

#### **4. Concluding remarks**

The present study, based on 52 years of data, brings out three important aspects of SST variability such as (1) decadal cycle in SST riding over a linear warming trend until 1995, (2) disruption in decadal cycle after 1995, and (3) a post-1995 slowdown in SST warming. The reasons for the observed variability was a combination of factors such as weakening of the link between SST and sunspot number after 1995, and the increase in the occurrence of cyclonic systems in the BoB post-1995 leading to an increase in the mixing of cold subsurface waters with warm surface waters. Although the cyclones are very intense in terms of air-sea interaction, they are temporally short lived. However, the oceanic mixing process triggered by them could impact the SST for a longer time. The cooling in the case of Cyclone Nargis lasted at least a fortnight. Thus, the BoB can cool twice a year during spring-summer and fall-winter periods through episodic occurrence of cyclonic systems. This cyclone-induced cooling of the upper waters of the BoB will increase with enhanced occurrence of the numbers of cyclonic systems, which in turn leads to a slowdown in the rise of the basin-wide SST. However, it is not clear how long will the present trend of slowdown in SST warming continue in the BoB. The greatest challenge lies in the quantification of the observed variability and the uncertainty associated with it. Equally challenging is to

decipher how these changes will impact the regional food and water security as most of the agriculture in this part of the world profoundly depends on the monsoon/ cyclonic system-driven rainfall.

### **Acknowledgements**

The authors wish to acknowledge Director, CSIR-National Institute of Oceanography (CSIR-NIO), Dona Paula, Goa as well as Council of Scientific and Industrial Research (CSIR), New Delhi for all the support and encouragement. JRD'M acknowledges CSIR for the fellowship. This is NIO contribution number xxxx.

### **Supporting Information**

Supporting information is present in S1 and S2. S1 describes the PWP model and the data used to force the model and for the initial conditions and also the MLD data, which is used to compare with the resultant MLD. S2 describes the peaking of the wind speeds and the resultant MLDs obtained.

### **References**

- Chen X, Tung K-K, 2014. Varying planetary heat sink led to global-warming slowdown and acceleration. *Science* **345**: 897–903. doi:10.1126/science.1254937.
- Holte J, Talley L, 2009. A New Algorithm for Finding Mixed Layer Depths with Applications to Argo Data and Subantarctic Mode Water Formation. *Journal of Atmospheric and Oceanic Technology* **26**: 1920–1939. doi:10.1175/2009JTECHO543.1.
- Holte J, Gilson J, Talley L, Roemmich D, 2010. Argo Mixed Layers, Scripps Institution of Oceanography/UCSD. <http://mixedlayer.ucsd.edu>, accessed 15<sup>th</sup> October, 2014.
- Kalnay E, Kanamitsu M, Kistler R, Collins W, Deaven D, Gandin L, Iredell M, Saha S, White G, Woolen J, Zhu Y, Leetmaa A, Reynolds R, Chelliah M, Ebisuzaki W, Higgins W, Janowiak J, Mo KC, Ropelewski C, Wang J, Jenne R, Joseph D, 1996. The NCEP/NCAR 40-year reanalysis project. *Bulletin of the American Meteorological Society* **77**: 437–470. doi: [http://dx.doi.org/10.1175/1520-0477\(1996\)077<0437:TNYRP>2.0.CO;2](http://dx.doi.org/10.1175/1520-0477(1996)077<0437:TNYRP>2.0.CO;2).
- Keeling CD, Piper SC, Bacastow RB, Wahlen M, Whorf TP, Heimann M, Meijer HA, 2001. Exchanges of atmospheric CO<sub>2</sub> and <sup>13</sup>CO<sub>2</sub> with the terrestrial biosphere and oceans from 1978 to 2000. I. Global aspects, SIO Reference Series, No. 01-06. Scripps Institution of Oceanography, San Diego.
- Keerthi MG, Lengaigne M, Vialard J, de Boyer Montégut C, Muraleedharan PM, 2013. Interannual variability of the Tropical Indian Ocean mixed layer depth. *Climate Dynamics* **38**: 1–17. doi:10.1007/s00382-012-1295-2.
- Kosaka Y, Xie S-P, 2013. Recent global-warming hiatus tied to equatorial Pacific surface cooling. *Nature* **501**: 403–407. doi:10.1038/nature12534.

- McCreary JP, Kundu PK, Molinari RL, 1993. A numerical investigation of dynamics, thermodynamics and mixed-layer processes in the Indian Ocean. *Progress in Oceanography* **21**: 181–244.
- McGregor S, Timmermann A, Stuecker MF, England MH, Merrifield M, Jin F-F, Chikamoto Y, 2014. Recent Walker circulation strengthening and Pacific cooling amplified by Atlantic warming. *Nature Climate Change* **4**: 888–892. doi:10.1038/nclimate2330.
- Narvekar J, Prasanna Kumar S, 2006. Seasonal variability of the mixed layer in the central Bay of Bengal and associated changes in nutrients and chlorophyll. *Deep-Sea Research Part I* **53**: 820–835.
- Narvekar J, Prasanna Kumar S, 2014. Mixed layer variability and chlorophyll a biomass in the Bay of Bengal. *Biogeosciences* **11**: 3819–3843.
- Potemra JT, Luther ME, O'Brien JJ, 1991. The seasonal circulation of the upper ocean in the Bay of Bengal. *Journal of Geophysical Research* **96**: 12667–12683.
- Prasad TG, 1997. Annual and seasonal mean buoyancy fluxes for the tropical Indian Ocean. *Current Science* **73**: 667–674.
- Prasanna Kumar S, Prasad TG, 1996. Winter cooling in the northern Arabian Sea. *Current Science* **71**: 834–841.
- Prasanna Kumar S, Narvekar J, 2005. Seasonal variability of the mixed layer in the central Arabian Sea and its implication on nutrients and primary productivity. *Deep-Sea Research Part II* **52**: 1848–1861.
- Prasanna Kumar S, Roshin RP, Narvekar J, Dinesh Kumar PK, Vivekanandan E, 2009. Response of the Arabian Sea to global warming and associated regional climate shift. *Marine Environmental Research* **68**: 217–222.
- Price JF, Mooers CNK, van Leer JC, 1978. Observation and simulation of storm-induced mixed-layer deepening. *Journal of Physical Oceanography* **8**: 582–599.
- Price JF, Weller RA, Pinkel R, 1986. Diurnal cycling: Observations and models of the upper ocean response to diurnal heating, cooling, and wind mixing. *Journal of Geophysical Research* **91**: 8411–8427.
- Rao RR, Sivakumar R, 2000. Seasonal variability of near-surface thermal structure and heat budget of the mixed layer of the tropical Indian Ocean from a new global ocean temperature climatology. *Journal of Geophysical Research* **105**: (C1), 995–1015. doi:10.1029/1999JC900220.
- Rao RR, Sivakumar R, 2003. Seasonal variability of sea surface salinity and salt budget of the mixed layer of the north Indian Ocean. *Journal of Geophysical Research* **108**: (C1), 3009. doi:10.1029/2001JC000907.
- Reynolds RW, Smith TM, Liu C, Chelton DB, Casey KS, Schlax MG. 2007. Daily High-resolution Blended Analyses for sea surface temperature. *Journal of Climate* **20**: 5473–5496. doi: http://dx.doi.org/10.1175/2007JCLI1824.1.
- Rupa Kumar K, Krishna Kumar K, Ashrit RG, Patwardhan SK, Pant GB, 2002. Climate Change in India: Observations and Model Projections, NATCOM Book on Climate Change, in: Shukla, P.R.,

Sharma, S., Raman, P.V. (Eds.), *Climate Change and India - Issues, concerns and opportunities*. Tata McGraw-Hill Publishing Co. Ltd.: New Delhi, India.

Schott FA, McCreary JP, 2001. The monsoon circulation of the Indian Ocean. *Progress in Oceanography* **51**: 1–123. doi: 10.1016/S0079-6611(01)00083-0.

Shankar D, Vinayachandran PN, Unnikrishnan AS, 2002. The monsoon currents in the north Indian Ocean. *Progress in Oceanography* **52**: 63–120.

Shetye SR, Shenoi SSC, Gouveia AD, Michael GS, Sundar DS, Nampoothiri G, 1991. Wind-driven coastal upwelling along the western boundary of the Bay of Bengal during the south-west monsoon. *Continental Shelf Research* **11**: 1397–1408.

Shetye SR, Gouveia AD, Shankar D, Shenoi SSC, Vinayachandran PN, Sundar D, Michael GS, Nampoothiri G, 1996. Hydrography and circulation in the western Bay of Bengal during the northeast monsoon. *Journal of Geophysical Research* **101**: 14011–14025.

Solar Influences Data analysis Centre (SIDC) team, 2012. *Monthly Report on the International Sunspot Number*, online catalogue of the sunspot index: <http://www.sidc.be/sunspot-data/>, '1749-2011'. World Data Center for the Sunspot Index, Royal Observatory of Belgium, Brussels, Belgium.

Subramanian V, 1993. Sediment load of Indian Rivers. *Current Science* **64**: 928–930.

Trenberth KE, Fasullo JT, 2013. An apparent hiatus in global warming? *Earth's Future* **1**: 19–32. doi: 10.1002/2013EF000165.

Trenberth KE, Fasullo JT, Branstator G, Phillips AS, 2014. Seasonal aspect of the recent pause in surface warming. *Nature Climate Change* **4**: 911–916. doi:10.1038/nclimate2341.

Varkey MJ, Murty VSN, Suryanarayana A, 1996. Physical oceanography of the Bay of Bengal and Andaman Sea. *Oceanography and Marine Biology- An Annual Review* **34**: 1–70.

Vinayachandran PN, Yamagata T, 1998. Monsoon response of the sea around Sri Lanka: Generation of thermal domes and anticyclonic vortices. *Journal of Physical Oceanography* **28**: 1946–1960.

Webster PJ, Holland GJ, Curry JA, Chang H-R, 2005. Changes in Tropical Cyclone Number, Duration, and Intensity in a Warming Environment. *Science* **309**: 1844–1846.

White WB, Lean J, Cayan DR, Dettinger MD, 1997. Response of global upper ocean temperature to changing solar irradiance. *Journal of Geophysical Research* **102**: (C2), 3255–3266. doi:10.1029/96JC03549.

Willson RC, Hudson HS, 1988. Solar luminosity variation in solar cycle 21. *Nature* **332**: 810–812. doi: 10.1038/33281OaO.

Woodruff SD, Diaz HF, Worley SJ, Reynolds RW, Lubker SJ, 2005. Early ship observational data and ICOADS. *Climatic Change* **73**: 169–194. doi:10.1007/s10584-005-456-3.

Yu L, Jin X, Weller RA, 2008. Multidecade Global Flux Datasets from the Objectively Analyzed Air-sea Fluxes (OAFlux) Project: Latent and sensible heat fluxes, ocean evaporation, and related surface meteorological variables, in: Woods Hole Oceanographic Institution, OAFlux Project Technical Report, OA-2008-01, 64 pp. Woods Hole Oceanographic Institution: Woods Hole, Massachusetts, U.S.A.

## Tables

**Table 1** Bay of Bengal partial correlation coefficients (r) and significance levels, between the 60-month running mean of SST and the 60-month running mean of the various parameters, viz. the net heat flux (NHF), wind speed (i.e. momentum flux), evaporation precipitation difference (E-P) (i.e. freshwater flux) and the number of DCS, in different periods. Both partial correlation and significance levels values are in bold-face, when significance level is greater than 99.99 %.

Partial Correlation	Period	NHF		Wind Speed		Number of DCS		E-P	
		r	Significance level (%)	r	Significance level (%)	r	Significance level (%)	r	Significance level (%)
SST	1960-2011	<b>0.53</b>	<b>&gt;99.99</b>	<b>0.56</b>	<b>&gt;99.99</b>	<b>-0.26</b>	<b>&gt;99.99</b>	-0.10	97.62
	1960-1995	<b>0.60</b>	<b>&gt;99.99</b>	<b>0.47</b>	<b>&gt;99.99</b>	-0.14	99.44	<b>-0.59</b>	<b>&gt;99.99</b>
	1995-2011	0.29	99.98	0.17	99.13	<b>-0.59</b>	<b>&gt;99.99</b>	0.25	99.89

**Table 2** Bay of Bengal (BoB) partial correlation coefficients (r) and significance levels, between the 60-month running mean of SST and 60-month running mean of the international sunspot number, 60-month running mean of the global CO<sub>2</sub> concentration and 60-month running mean of the BoB number of DCS, in different periods. Both partial correlation and significance level values are in bold face, when significance level is greater than 99.99 %.

Partial Correlation	Period	Sunspot Number		CO <sub>2</sub> concentration		Number of DCS	
		r	Significance level (%)	r	Significance level (%)	r	Significance level (%)
SST	1960-2011	<b>0.74</b>	<b>&gt;99.99 %</b>	<b>0.88</b>	<b>&gt;99.99%</b>	<b>-0.18</b>	<b>&gt;99.99%</b>
	1960-1995	<b>0.76</b>	<b>&gt;99.99%</b>	<b>0.47</b>	<b>&gt;99.99%</b>	<b>-0.26</b>	<b>&gt;99.99%</b>
	1995-2011	0.2	99.03%	<b>0.82</b>	<b>&gt;99.99%</b>	<b>-0.43</b>	<b>&gt;99.99%</b>

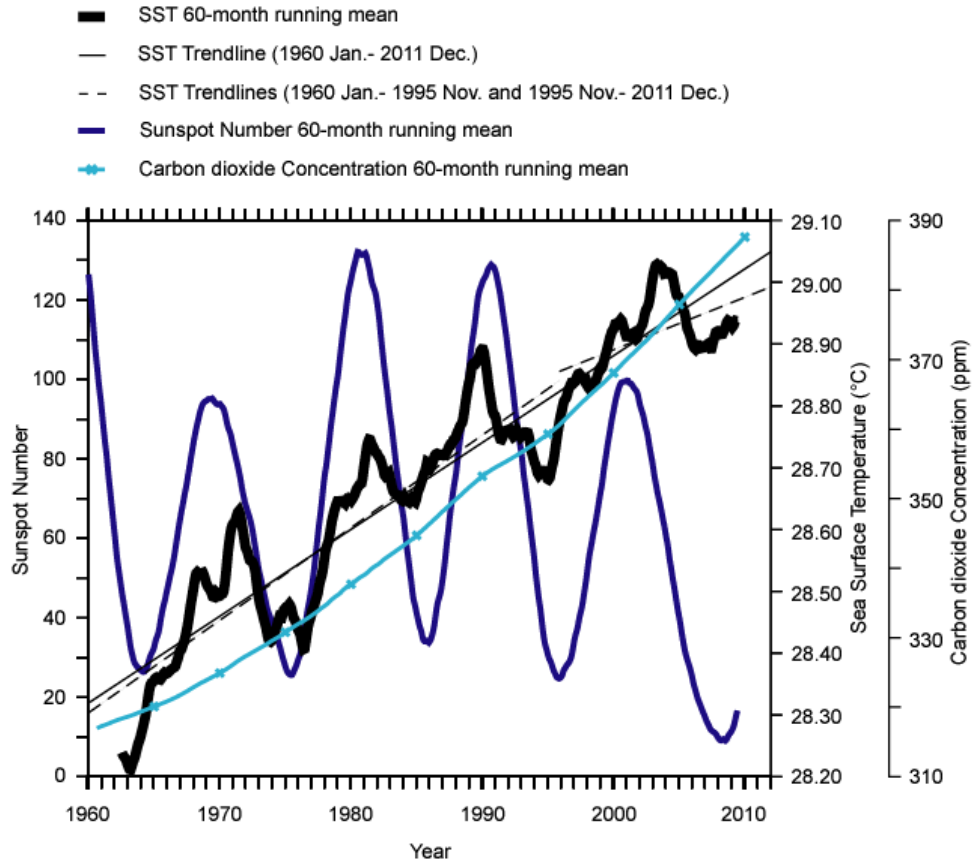


**Figure 1** Basin-averaged 60-month running means of Bay of Bengal (Eq. to 25 °N, 80 °E to 99 °E) SST (thickest line, black), international sunspot number (thick line, blue) and carbon dioxide concentration (thick line with cross-marks, light-blue) for the period 1960 January to 2011 December. SST trendline for the entire period of study (thin line, black) and pre-1995 and post-1995 SST trendlines (thin dashed lines, black) are also shown.

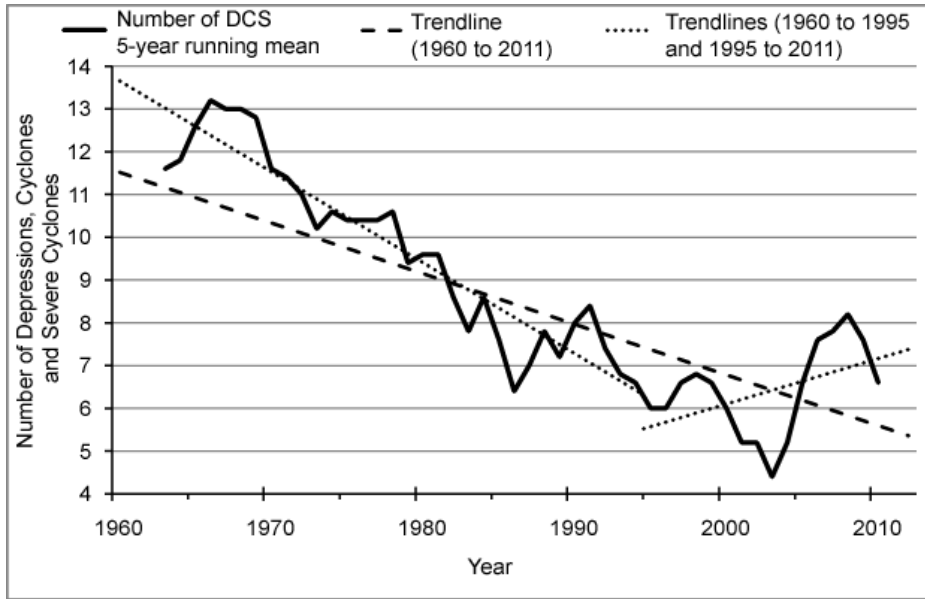


**Figure 2** Five-year running mean of the total number of DCS in the Bay of Bengal (Eq. to 25 °N, 80 °E to 99 °E) (thick line, black) for the period from 1960 to 2011. Trendlines for the entire period of study (dashed line, black) and in the pre-1995 and post-1995 periods (dotted lines, black) are also shown.

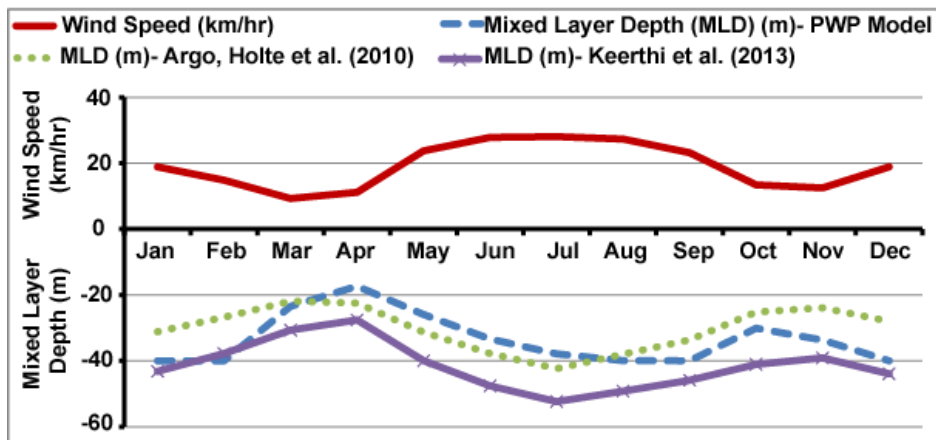


**Figure 3** Seasonal cycle of wind speed (m/s) (red thick line) and mixed-layer depths (m) in the Bay of Bengal from PWP-model (blue dashed line), Holte et al. (2010) (green dotted line) and Keerthi et al. (2013) (purple thick line with cross marks).

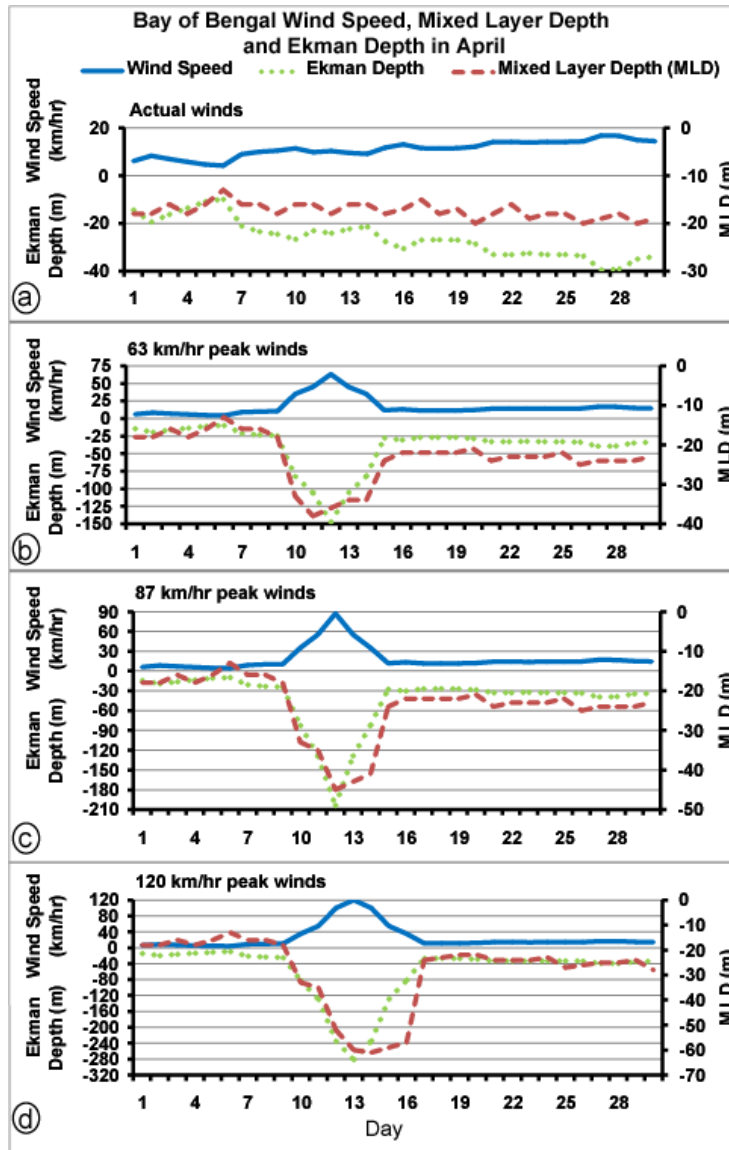


**Figure 4** Bay of Bengal wind speeds (km/hr; blue solid line), Ekman depths (m; green dotted line) and mixed-layer depths (m, red dashed lines) for actual wind speeds (Panel a), model wind speeds peaking to 63 km/hr (Panel b), model wind speeds peaking to 87 km/hr (Panel c) and model wind speeds peaking to 120 km/hr (Panel d), all in the month of April.



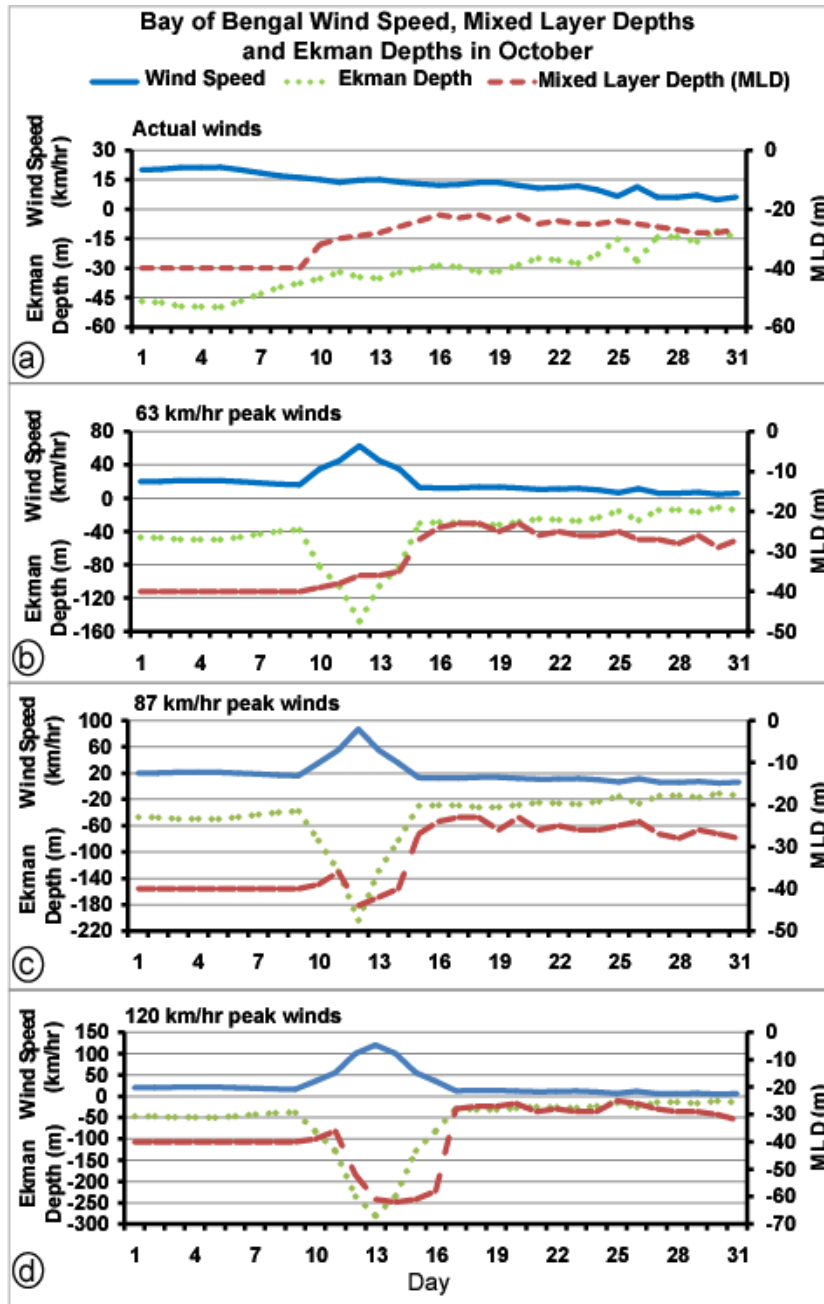


**Figure 5** Bay of Bengal wind speeds (km/hr; blue solid line), Ekman depths (m; green dotted line) and mixed-layer depths (m, red dashed lines) for actual wind speeds (Panel a), model wind speeds peaking to 63 km/hr (Panel b), model wind speeds peaking to 87 km/hr (Panel c) and model wind speeds peaking to 120 km/hr (Panel d), all in the month of October.

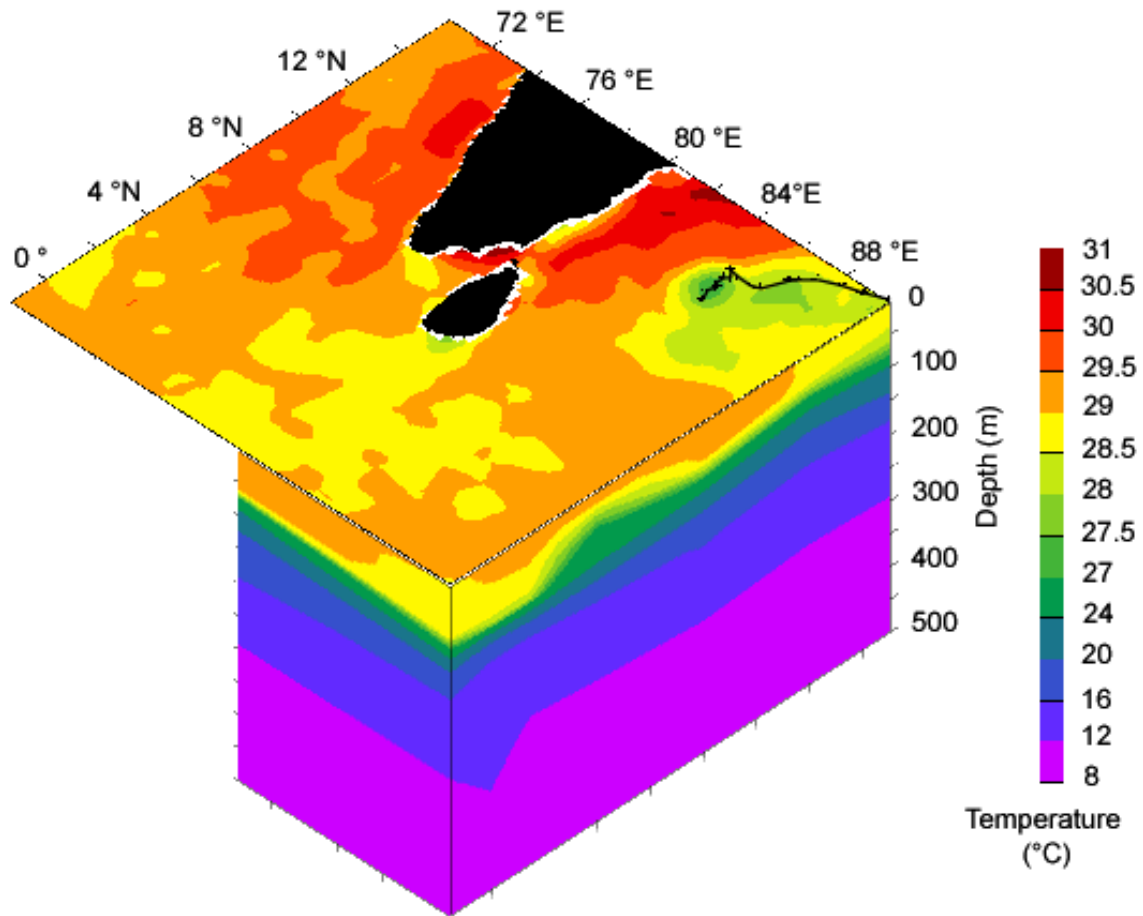


**Figure 6** Schematic showing the SST cooling associated with the passage of cyclone Nargis, which occurred during the period from the 27th of April to the 3rd of May 2008. The black solid line is the cyclone track and is plotted from the 27th of April to the 1st of May 2008, while the "x" marks denote the 6-hourly positions in this period. The SST data is on the 2nd of May 2008, from NOAA daily OISST and is obtained from <http://www.ncdc.noaa.gov/sst/griddata.php> (Reynolds et al., 2007). The vertical temperature data along the 90 °E (5-day average centred on the 2nd of May) and 1.5 °S (5-day average centred on the 3rd of May) sections (<http://www.pmel.noaa.gov/tao/disdell/frames/main.html>) are from Research moored Array for African-Asian-Australian Monsoon Analysis and prediction (RAMA) moorings. The cyclone track data is from [http://weather.unisys.com/hurricane/n\\_indian/2008H/NARGIS/track.dat](http://weather.unisys.com/hurricane/n_indian/2008H/NARGIS/track.dat)

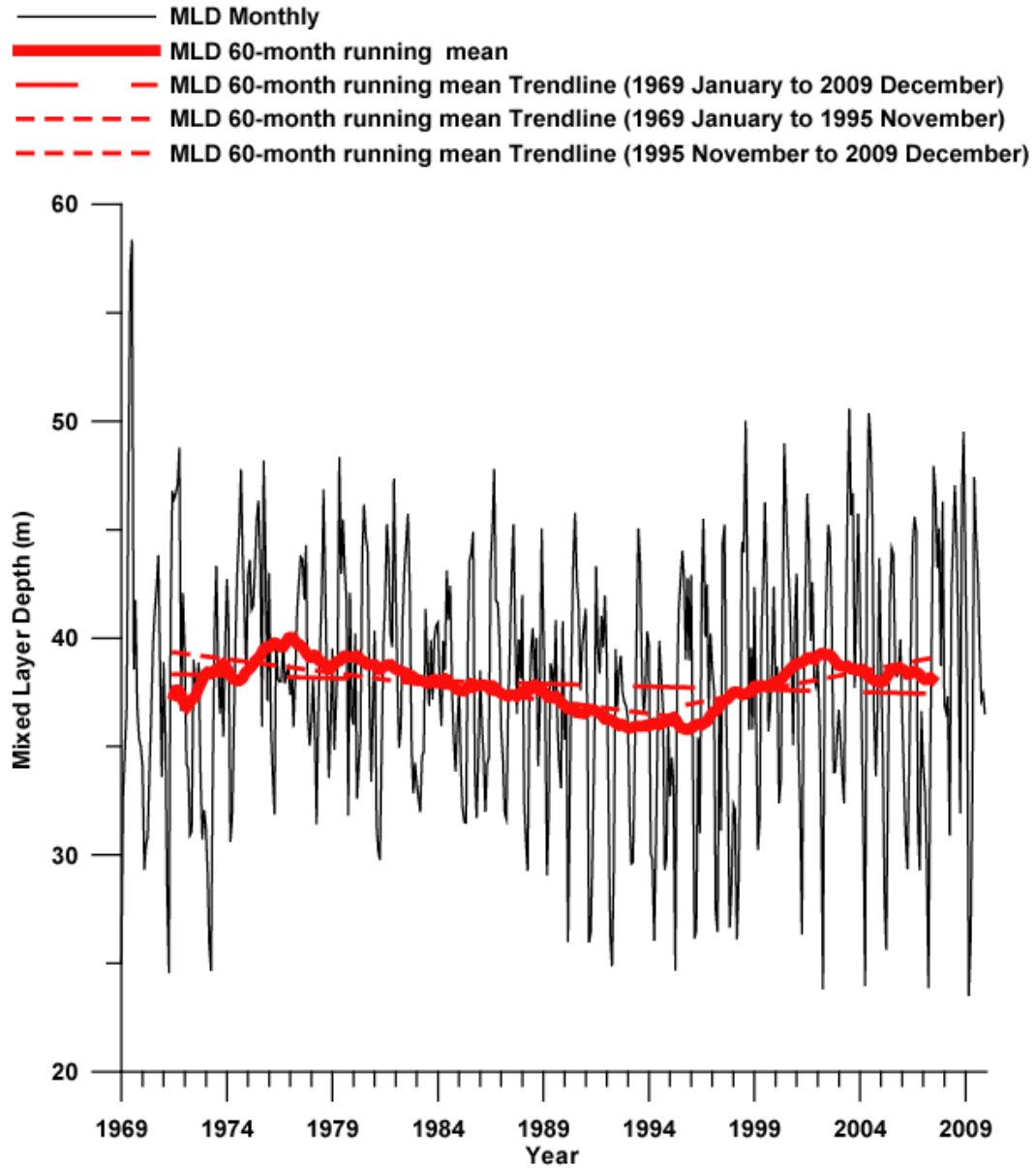


**Figure 7** Bay of Bengal (Eq.- 25 °N, 80 °E- 99 °E) basin-averaged mixed layer depth (MLD) in metres. Data plotted is monthly (black thin line), 60-month running mean (red thickest line), and 60-month running mean trendlines, in the periods from 1969 January to 2009 December (red, thick and large-dashed line) and from 1969 January to 1995 November and from 1995 November to 2009 December (both are red, thin and small-dashed lines).

## Supporting Information

### Why is the Bay of Bengal experiencing a reduced rate of sea surface warming?

Joshua Rosario D'Mello<sup>a</sup> and S. Prasanna Kumar<sup>a,\*</sup>

The Sea Surface Temperature (SST) in the Bay of Bengal is analysed in the period from 1960 January to 2011 December, and shows a decadal cycle riding on an increasing trend till 1995. In the post-1995 period, there is a disruption of the decadal cycle and an SST slowdown.

The SST decadal cycle is due to the sunspot number cycle, while the SST rise is due to the increasing CO<sub>2</sub> concentration in the atmosphere. The slowdown in the SST rise, in the post-1995 period, is due to the increase in the number of depressions, cyclones and severe cyclone (DCS). The cyclonic systems can cause mechanical mixing and cause the mixing of the mixed-layer waters with the cooler of the sub-surface waters, there-by reducing the SST.

This process of the deepening of the mixed-layer is shown through the Price Weller Pinkel (PWP) model. The increase in the SST by the atmospheric CO<sub>2</sub> concentration and the SST cooling due to the increasing number of depressions, cyclones and severe cyclones after-1995, are opposing processes. The SST in the Bay of Bengal is observed as a slowdown.

## S1

### S.1.1 Price-Weller-Pinkel (PWP) Model

The Price-Weller-Pinkel (PWP) model (Price *et al.*, 1986) is a mixed-layer model similar to the dynamic instability model of Price *et al.* (1978), but modified to include mixing in the stratified fluid, below the mixed-layer. The model takes into account mixing processes namely (1) free convection arising due to surface heat loss, (2) mixed-layer entrainment by relaxation and (3) shear flow instability driven mixing. Generally, mixing due to free convection in the BoB is very shallow and mostly confined to the upper few tens of centimetres of the water column. In contrast, the last two are the dominant processes that determine the depth of the mixed-layer and are related to momentum flux by the wind through the Richardson number.

Since the vertical mixing of the water is caused by changes in the density due to the changes in the net heat and fresh water fluxes and momentum flux they were calculated from zonal and meridional wind stress components, shortwave and longwave radiations, latent and sensible heat fluxes, evaporation, precipitation and riverine discharge, riverine runoff and catchment area data. The model was initialized with the climatological temperature and salinity profiles and the daily fluxes were used to force the model. The model was run for 730 days (2 years), with a time step of 86400 seconds (1 day) and with a vertical grid interval of 1 m.

### S.1.2 Data for the Model

The daily wind stress components were obtained from [http://apdrc.soest.hawaii.edu/dods/public\\_data/satellite\\_product/ifremer/daily\\_flux](http://apdrc.soest.hawaii.edu/dods/public_data/satellite_product/ifremer/daily_flux), while the daily evaporation data was obtained from [ftp://ftp.whoi.edu/pub/science/oaflux/data\\_v3/daily/evaporation/](ftp://ftp.whoi.edu/pub/science/oaflux/data_v3/daily/evaporation/). The daily rainfall data was obtained from <http://apdrc.soest.hawaii.edu/dchart/index.html?dset=a2c287de3ad7cab9999e50371916fe>. The daily riverine discharge, run-off and catchment area data for the rivers Sittang, Irrawaddy, Chindwin, Brahmaputra, Ganges, Damodar, Subarnarekha, Godavari, Krishna, Penner and Cauvery were obtained from <http://www.compositerunoff.sr.unh.edu> (Fekete *et al.*, 2000). Similarly, for the rivers Mahanadi, Ponnaiyar, Vaigai, Mahaveli Ganga and Gin Ganga the riverine discharge, riverine runoff and catchment area data were obtained from [http://www.sage.wisc.edu/riverdata/scripts/station\\_table.php?qual=32&filenum=1114](http://www.sage.wisc.edu/riverdata/scripts/station_table.php?qual=32&filenum=1114). The fore-mentioned website gave data for the riverine discharge and runoff data of the river Brahmani, but the catchment area was taken from Vaithiyanathan *et al.* (1988).

The daily downward solar radiation flux and upward long wave radiation flux were obtained from <http://www.esrl.noaa.gov/psd/data/gridded/data.ncep.reanalysis.derived.otherflux.html>, while the daily latent heat flux and sensible heat flux data were obtained from <http://oaflux.whoi.edu>.

Temperature (Locarnini *et al.*, 2010) and salinity (Antonov *et al.*, 2010) profile data were taken from World Ocean Atlas 2009 available at [http://www.nodc.noaa.gov/OC5/WOA09/netcdf\\_data.html](http://www.nodc.noaa.gov/OC5/WOA09/netcdf_data.html). For comparing the model MLD, the data on the mixed-layer depths were taken from Holte *et al.* (2010) (<http://mixedlayer.ucsd.edu/data/monthlyclim.nc>) and Keerthi *et al.* (2013) ([http://www.ifremer.fr/cerweb/deboyer/mld/Surface\\_Mixed\\_Layer\\_Depth.php](http://www.ifremer.fr/cerweb/deboyer/mld/Surface_Mixed_Layer_Depth.php)). In Holte *et al.* (2010)

the MLD climatology was computed using Argo profiles and a hybrid method (Holte and Talley, 2009), while in Keerthi *et al.* (2013) the monthly MLD data for the Indian Ocean, during 1969 to 2009 was based on temperature and salinity profiles taken from different sources namely National Oceanographic Data Centre (NODC) World Ocean Database 2009 (WOD 09), World Ocean Circulation Experiment (WOCE) global dataset version 3.0, Argo profile data and Tropical Atmosphere Ocean project Research moored Array for the African-Asian-Australian Monsoon Analysis and prediction (TAO RAMA) buoy daily data. Using this data monthly mean climatology (1969-2009) was computed for comparing with PWP model output.

## S2

### S2.1 PWP model wind speeds in April (spring- summer transition)

The cyclonic winds were introduced in a stepped manner from the 10<sup>th</sup> of April so as to attain the peak value on the 12<sup>th</sup> of April (runs 1 and 2, having peak values of 63 km/hr and 87 km/hr respectively) and the 13<sup>th</sup> of April (run 3, having a peak value of 120 km/hr). The model output was analyzed and the maximum mixed-layer depths were found to be 41 m (run 1, Panel b in Figure 4), 45 m (run 2, Panel c in Figure 4) and 61 m (run 3, Panel d in Figure 4) respectively (Figure 4). Note that in April the model MLD was 17 m when forced with the actual winds of 11 km/hr (Panel a in Figure 4).

### S2.2 PWP model wind speeds in October (fall- winter transition)

The model was forced with increasing winds in a stepped manner from 10<sup>th</sup> October so as to attain peak value of 63 km/hr (run 1, Panel b in Figure 5) and 87 km/hr (run 2, Panel c in Figure 5) on 12<sup>th</sup> October and 120 km/hr (run 3, Panel d in Figure 5) on 13<sup>th</sup> October. The model MLDs were found to be 38 m (run 1), 44 m (run 2) and 62 m (run 3) respectively, while it was 30m when forced with actual winds of 13 km/hr (Panel a in Figure 5).

## References

- Antonov JI, Seidov D, Boyer TP, Locarnini RA, Mishonov AV, Garcia HE, Baranova OK, Zweng MM, Johnson DR, 2010. World Ocean Atlas 2009, Volume 2: Salinity, in: Levitus S, *NOAA Atlas NESDIS 69*. U.S. Government Printing Office: Washington, D.C., U.S.A.
- Fekete BM, Vorosmarty CJ, Grabs W, 2000. *Global Composite Runoff Fields based on observed river discharge and simulated water balances*. Global Runoff Data Centre, Koblenz, Germany.
- Holte J, Talley L, 2009. A New Algorithm for Finding Mixed Layer Depths with Applications to Argo Data and Subantarctic Mode Water Formation. *Journal of Atmospheric and Oceanic Technology* **26**: 1920–1939. doi:10.1175/2009JTECHO543.1.
- Holte J, Gilson J, Talley L, Roemmich D, 2010. Argo Mixed Layers, Scripps Institution of Oceanography/UCSD. <http://mixedlayer.ucsd.edu>, accessed 15<sup>th</sup> October, 2014.
- Keerthi MG, Lengaigne M, Vialard J, de Boyer Montégut C, Muraleedharan PM, 2013. Interannual variability of the Tropical Indian Ocean mixed layer depth. *Climate Dynamics* **38**: 1–17. doi:10.1007/s00382-012-1295-2.
- Locarnini RA, Mishonov AV, Antonov JI, Boyer TP, Garcia HE, Baranova OK, Zweng MM, Johnson DR, 2010. World Ocean Atlas 2009, Volume 1: Temperature, in: Levitus, S., *NOAA Atlas NESDIS 68*. U.S. Government Printing Office: Washington, D.C.
- Price JF, Mooers CNK, van Leer JC, 1978. Observation and simulation of storm-induced mixed-layer deepening. *Journal of Physical Oceanography* **8**: 582–599.
- Price JF, Weller RA, Pinkel R, 1986. Diurnal cycling: Observations and models of the upper ocean response to diurnal heating, cooling, and wind mixing. *Journal of Geophysical Research* **91**: 8411–8427.
- Vaithyanathan P, Ramanathan AL, Subramanian V, 1988. Erosion, Transport and Deposition of sediments by the tropical rivers of India. *Sediment Budgets* **174**: 561–574.